

Counting and Breaking Individual Biological Bonds: Force Spectroscopy of Tethered Ligand-Receptor Pairs

Raymond W. Friddle[†], Todd A. Sulchek[†], Huguette Albrecht[‡], Sally J. De Nardo[‡] and Aleksandr Noy^{†,*}

[†]Chemistry and Materials Sciences Directorate, Lawrence Livermore National Laboratory, Livermore, CA 94550

[‡]Radiodiagnosics and Therapy, UC Davis Cancer Center, University of California Medical Center, Sacramento, CA 95817

Abstract: Force spectroscopy provides a direct approach for probing biological interactions at the single-molecule level. Tethered systems, in which flexible polymer linkers connect the interacting molecules to the surfaces of the atomic force microscope probe and sample, provide a particularly attractive platform for studying such interactions. We will review the basic physical principles of force spectroscopy measurements in these systems, and show that mechanical properties of the tether linkages allow independent determination of the bond rupture forces and the number of ruptured bonds. Forces measured in these systems obey the predictions of a Markovian model for the strength of multiple parallel bonds. Finally, we discuss the use of the dynamic force spectra of single and multiple protein-ligand bonds for determination of kinetic parameters for multivalent interactions.

INTRODUCTION: TETHERED SYSTEMS IN FORCE SPECTROSCOPY

Interactions between biological molecules drive the overwhelming majority of cellular processes and span a wide range of strength and complexity. Often a number of individual bonds between receptor-ligand pairs combine to produce much stronger interactions that allow organisms to perform biological functions that generate complex stresses and involve substantial molecular rearrangements. Such interactions play an important role in adaptive immune response [1] and intercellular adhesion [2]. Complex bonds are also featured in the mechanism of action of many pharmaceuticals [3] as well as serve as a generic affinity-enhancing approach [4, 5] in a variety of therapies and imaging techniques that target specific biological tissues [6, 7].

The last decade saw an emergence of a number of interaction force measurement techniques that allowed researchers to measure and apply molecular level stresses [8-10]. These methods can probe binding on the single molecule level. This is an advantage over ensemble-based techniques which suffer from spatial and temporal averaging that can obscure the details of the interaction [11-14]. In particular, Atomic Force Microscopy (AFM) probes ligand-receptor interactions by simply pulling off the ligand from the receptor using external force applied by a flexible cantilever [15]. In a typical force spectroscopy experiment the bond strength is defined by the force that produces the most frequent bond failure in repeated tests of bond breakage on a given timescale [16]. Further refinements of the technique based on kinetic approaches, such as Dynamic Force Spectroscopy (DFS), allowed researchers to quantify kinetic off-rates and the distances to transition states [16].

The main conceptual difficulties in performing and interpreting bond strength measurements on the single molecule scale are: (a) the necessity to separate the specific interactions from the non-specific interactions of the probe tip and sample and (b) the absence of a reliable way to determine the number of interacting molecules independent of the binding force values. In general, force spectroscopy does not provide an immediate way to discriminate between the receptor-ligand bond or non-specific tip-surface interactions, therefore researchers have to address specificity by passivating the sample and probe surfaces and by using careful control experiments. Determination of the number of interacting bonds is equally challenging. Of the three main force spectroscopy techniques- atomic force microscopy (AFM), [9] surface forces apparatus (SFA) [17] and optical tweezers [18] – only SFA provides independent contact area assessment; yet the contact area in the SFA measurements tends to be large and thus makes it difficult to probe a limited number of bonds. Determination of the number of the interacting bonds solely by measuring rupture force with AFM or optical tweezers is equally problematic since stochastic rupture [19] and variation in the bond load rate [16] typically produce overlapping binding force distributions.

A particular approach to the force spectroscopy measurements based on linking the interacting molecules to the surfaces of an AFM tip and sample with long flexible polymer tethers (Fig. 1) provides a simple and powerful solution to the two problems that we discussed in the previous paragraph. First, the tethers spatially isolate non-specific probe-sample interactions from the specific interactions of the tethered molecules; the specific interactions now occur at a fixed tip-sample distance given by the combined length of the two polymer tethers (Fig. 2C). Second, if the length of the tethers is much larger than the polymer persistence length [20] they remain truly flexible, allowing the necessary conformational freedom to maximize the efficiency of the ligand-receptor docking. Third, this

*Address correspondence to this author at the Chemistry and Materials Sciences Directorate, Lawrence Livermore National Laboratory, Livermore, CA 94550; Tel: 925-424-6203; Fax: 925-422-9298; E-mail: noy1@llnl.gov

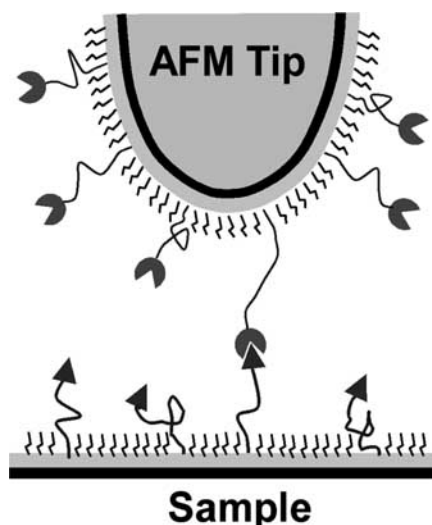


Fig. (1). Schematic of a force spectroscopy experiment in a tethered system. Both interacting molecules are connected to the surfaces of the AFM tip and sample with long flexible polymer chains.

configuration separates the binding pair from the surfaces of the tip and sample, thus allowing the bond to rupture in an environment that closely resembles a solution environment. Fourth, as we will demonstrate, tethered systems provide a convenient way to determine the number of the interacting bonds independent of the magnitude of the rupture force.

Finally, tethered systems provide a nearly-ideal experimental system for dynamic force spectroscopy measurements, as tether elasticity provides a means for very efficient rebinding suppression.

In this article we first review the non-linear elastic behavior of a polymer tether under load, that is central for quantitative interpretation of force spectroscopy measurements and then briefly discuss how these properties modify the kinetics of bond rupture under an external load. We then show how force spectroscopy of tethered systems can determine how the rupture strength of multiple bonds scales with the number of bonds. Finally, we discuss the dynamic force spectroscopy of multiple individual protein-antibody bonds.

Elasticity of a Polymer Chain Under External Loading Force

Entropic Elasticity of a Polymer Chain

Solvent molecules moving in random directions constantly bombard a polymer chain in solution; this constant jostling of the chain supplies the thermal energy that helps the polymer molecule to adopt a coiled configuration that maximizes its entropy. If we attempt to stretch the polymer beyond this entropically-favored configuration, the polymer chain will resist the stretching, producing a force that acts in the direction opposite to the external force. As we stretch the chain closer to its contour length the resistance gets stronger as the number of

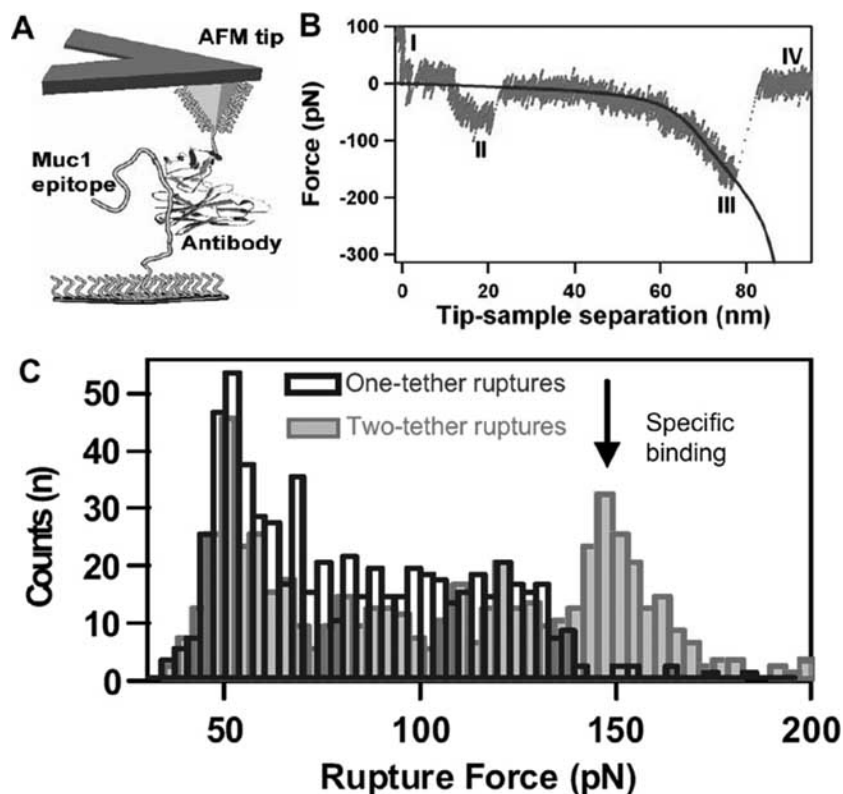


Fig. (2). **A.** Schematics of the tethered system for interactions of peptide MUC1 with the antibody fragment recognizing MUC1. **B.** Representative force vs. distance trace measured in this system. Solid line indicate a fit of the tether extension trace to the TLS-eFJC model (Eq. 3 and 5) **C.** Histograms of the rupture forces measured in the one linker length rupture region (filled bars) and two linker lengths rupture region (unfilled bars). An arrow indicates the peak corresponding to the specific peptide-antibody interactions.

configurations accessible to the system decreases: a polymer chain stretched beyond its natural conformation behaves as a non-hookean “entropic” spring.

Most of the common models that describe the behavior of polymers can be derived from the Kratky-Porod’s [21] description of a chain of N rigid segments under a tension F along the z axis,

$$H = -\frac{B}{a} \sum_{i=2}^N \hat{a}_i \cdot \hat{a}_{i-1} - Fa \sum_{i=1}^N \hat{a}_i \cdot \hat{z} \quad (1)$$

where H is the Hamiltonian of the system, with segment lengths a , bending modulus B , and segment unit vectors \hat{a}_i . The configurational partition function Z is then calculated as the Boltzmann weighted sum over the chain orientations \hat{a}_i . Under a constant force F the average extension of the molecule along the z axis $\langle z \rangle$ is then given by the rate of change of the free energy: $\langle z \rangle = d(k_B T \ln Z) / dF$. One of the limiting cases of Eq. 1, the freely jointed chain (FJC) is very useful for the description of polymer stretching in tethered force spectroscopy measurements.

The FJC model describes a polymer consisting of rigid segments ($B = 0$) that are free to rotate about their connections. The only parameter that governs the polymer’s response to an external force is the Kuhn statistical segment length a . This length is related to the persistence length P , of the polymer by $a = 2P$. The FJC model predicts that the mean extension $\langle z \rangle$ under constant force F follows a Langevin function:

$$\langle z \rangle = Na \left(\coth \frac{Fa}{k_B T} - \frac{k_B T}{Fa} \right) \quad (2)$$

Note that as the extension of the polymer approaches its contour length, the force approaches infinity. A more realistic extension of the FJC model allows for elastic stretching of the backbone in the high force regime:

$$\langle z \rangle = Na \left(\coth \frac{Fa}{k_B T} - \frac{k_B T}{Fa} \right) \left(1 + \frac{F}{K_s} \right) \quad (3)$$

where K_s is the stretching modulus of the polymer.

Force-Induced Transitions within the Polymer Chain

Often the effect of an external load goes beyond simply straightening the polymer chain and causes internal conformational transitions. Unfolding of the Ig domains in a titin molecule [22] and conformational transitions in monomer subunits of PEG [23] represent examples of such conformational changes. Boltzmann partitioning of the states can elegantly model a polymer chain with subunits that undergo an equilibrium transition from a shortened state to a lengthened state [23],

$$\frac{N_f}{N_u} = \exp \frac{\Delta G - F \Delta z}{k_B T} \quad (4)$$

where $\Delta G = \Delta G_u^* - \Delta G_f^*$ is the energy difference between the folded and unfolded state at zero force, Δz is the length difference between the two states, and N_f and N_u are the number of domains in the folded and unfolded states. Note that similar to using pH or solution ionic strength to shifts the equilibrium in a chemical reaction, the applied force can tilt the energy landscape and change the relative equilibrium populations of the folded and unfolded states (Fig. 3B). Considering that $N = N_u + N_f$, it is straightforward to show that the fractional contribution of domains in the folded and unfolded states to the average length of the polymer is,

$$L_C(F) = N \left(\frac{N_u}{N} l_u + \frac{N_f}{N} l_f \right) = N \times \left(\frac{l_u}{\frac{\Delta G(F)}{k_B T} + 1} + \frac{l_f}{\frac{-\Delta G(F)}{k_B T} + 1} \right) \quad (5)$$

where $\Delta G(F) = \Delta G - F \Delta z$ is the force-tilted energy barrier, and l_u and l_f are the domain lengths when unfolded or folded respectively. Substitution of this equation in place of the contour length in the eFJC model produces the force-extension relationship for a generic polymer chain with segments that can undergo structural transitions under load. Eqs. 4 and 5 provide the main framework for describing the elastic response of polymer linkers such as PEG that are used extensively in force spectroscopy experiments.

Dynamics of Single Bond Rupture in Tethered Systems

The current description of the physics of non-covalent bond rupture originates from the framework proposed by Bell in the 1970s [19]. In this picture, external force lowers the energy barrier separating the bound state from the unbound state while the thermal fluctuations continuously try to drive the system over that barrier. In the absence of force, the intrinsic transition rate is small but external loading can cause exponential amplification of this rate and eventually leads to the quick breakage of the bond [16]. Since the stability of the bond is effected by fluctuations in the system, the nature of the linkage between the interacting molecular pair and the force transducer can have profound consequences for the bond rupture kinetics. According to Kramers’ description of thermally-activated transitions in an overdamped molecular system [24] the intrinsic rate of bond rupture is inversely proportional to the damping coefficient of the system. Note that this observation can have immediate practical consequences for force spectroscopy experiments: if the interacting molecule is connected rigidly to an AFM tip, the effective spontaneous rate of dissociation in this system could differ from the dissociation rate of the free molecule by orders of magnitude. For example, an AFM tip within 1 nm of a surface can have a damping coefficient as high as 10^{-4} kg/s in solution [25]. When compared to the damping coefficients of small molecules, which are typically

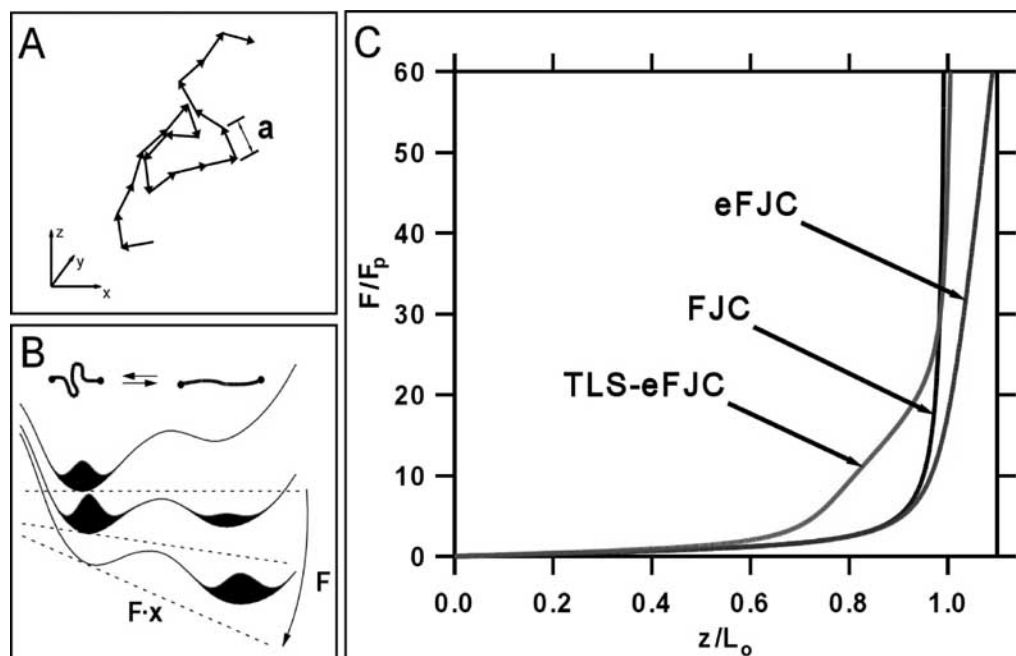


Fig. (3). A. Schematic representation of a Freely-Jointed Chain. B. Schematic representation and potential energy profiles of a two-level system under an external loading force F . C. Force-Extension profiles for Freely Jointed Chain (FJC), Extensible Freely-Jointed Chain (eFJC), and Freely-Jointed Chain with two-state conformation transition elements (TLS-eFJC). Forces are scaled by the characteristic force constant $F_p = k_B T/P$.

close to 10^{-11} kg/s, the difference in damping due to probe linkage can greatly decrease the spontaneous rate of dissociation (in this example by a factor of about 10^{-7} !). When a polymer linker separates the AFM tip and the molecule, the drag of the cantilever falls off with polymer length and gets replaced with the drag of the polymer molecule itself. If the macromolecules that form the chemical bond are substantially large, we can neglect the linker drag and assume that the dynamics will be dominated by the diffusion characteristics of the molecule [26]. In this case the force spectroscopy measurement will determine the intrinsic dissociation rate accurately.

An additional important consideration arises from an often-overlooked assumption in the Bell model (which has been carried over to most of the subsequent models of force spectroscopy experiments), that postulates that the forced rupture of a non-covalent bond is irreversible. In principle, this assumption is not always correct, as there is possibility of rebinding at slow loading. However, the non-Hookean shape of the potential for stretching a typical polymer tether ensures that at almost any applied force the stretched polymer molecule contracts sufficiently upon bond rupture and thus inhibits rebinding events over all experimentally accessible loading rates. In this case the bond ruptures are truly irreversible and tethered systems represent a nearly ideal realization for the first order kinetic process that is described by most of dynamic force spectroscopy models.

The inclusion of the non-linear tether spring between the bond and the force transducer modifies the loading regime encountered in the AFM measurements. Typically, the AFM instrument moves the force transducer away from the sample at a constant rate, producing a constant increase in the loading force. In a tethered system, even if the force

transducer moves at a constant rate, the bond is effectively stretched by the tether, and the loading force experienced by the bond does not increase linearly. Non-linear loading introduces substantial complications into the analysis of the rupture kinetics, and in general precludes their analytical solution. Fortunately Gaub and co-workers [27] showed that the loading rate can be replaced with an instantaneous loading rate at the moment of bond rupture without substantially altering the force spectrum for the bond; all data presented in this review have been analyzed using this procedure, which should be considered a standard practice for analyzing tethered systems.

COUNTING BIOLOGICAL BONDS: STRENGTH OF MULTIPLE LIGAND-RECEPTOR INTERACTIONS

Counting Individual Bonds

If we consider n_t identical parallel PEG tethers (each containing n_m monomers) the force-extension relationship for n_t PEG tethers will be:

$$L(F, n_t) = L_c(F, n_t) \cdot \left(\coth \left(\frac{Fa}{n_t k_B T} \right) - \frac{n_t k_B T}{Fa} \right) + \frac{n_m F}{n_t K_S} \quad (6)$$

where L_c is the force-dependent contour length given by Eq. 5, a is the Kuhn length, and K_S is the elastic constant. Typically, the tethers are much longer than any offset introduced by variations in the tether position on the probe tip; therefore we can consider all PEG linkers to have identical length. (The analysis of the rupture kinetics in cases where the tethers have different lengths is more complicated and we refer the reader to a previous publication [28]). The parameters for calculating this force-extension relationship

for PEG in aqueous solution were found by Oesterhelt *et al.* [23]. The model shows that PEG linker stiffness follows three distinct regions (see, for example, Fig. 4A). In the “soft” regime below 100 pN only the entropic forces contribute to the measured stiffness (region I). The stiffness at moderate forces between 100 and 300 pN represents breaking of water bridge-mediated helical structures and results in a relatively constant stiffness value (region II). High stiffness region III represents enthalpic stretching of the covalent bonds within each monomer. A comparison of the stretching profiles for multiple identical PEG tethers (Fig. 4A) shows that an increase in the number of tethers produces a characteristic stiffness increase in the intermediate regime (II). This difference in the force-extension profiles provides a *unique elastic signature* that identifies the number of tethers that produce a particular rupture trace. Fig. 4B-D shows that the measured single and multiple PEG tether extension traces fit this model very well, even if the model uses only a single parameter, n_m - the number of PEG monomers in each tether.

Strength of Multiple Peptide-Antibody Bonds

Significantly, this procedure allows us to identify the number of bonds corresponding to each of the large number of the specific rupture events measured for interactions of the tethered peptide Mucin 1 (MUC1) and the single-chain antibody fragment (scFv) recognizing the MUC1 peptide. Not surprisingly, these data (Fig. 5) show that an increase in the number of bonds results in the increase in the measured

rupture force. It is interesting to note that the measured force appears to increase nearly linearly with the number of bonds. Williams [29] has analyzed rupture of multiple identical bonds and showed that the measured rupture force F^* , should scale with the number of bonds N_B and the measured loading rate r_F , as:

$$r_F = k_{off} \frac{k_B T}{x_\beta} \left[\sum_{i=1}^{N_B} \frac{1}{i^2} \exp \left(-\frac{F^* x_\beta}{i k_B T} \right) \right]^{-1} \quad (7)$$

where x_β is the characteristic bond width, k_{off} is the thermodynamic off rate for a single bond and $k_B T$ is the thermal energy scale. The rupture forces that we calculated using Eq. 7 show reasonable agreement with the experimental data for the full range of loading rates used in the experiments (Fig. 5); however, all calculated curves show a more pronounced curvature than the experimental data for both high and low loading rates.

This deviation disappears, however, when we consider the details of the bond loading in a tethered system. As we discussed in the previous section, non-linear stiffness of PEG tethers and fluctuations in the binding force causes every rupture event to occur at a different instantaneous loading rate. The increase in the number of bonds produces stronger

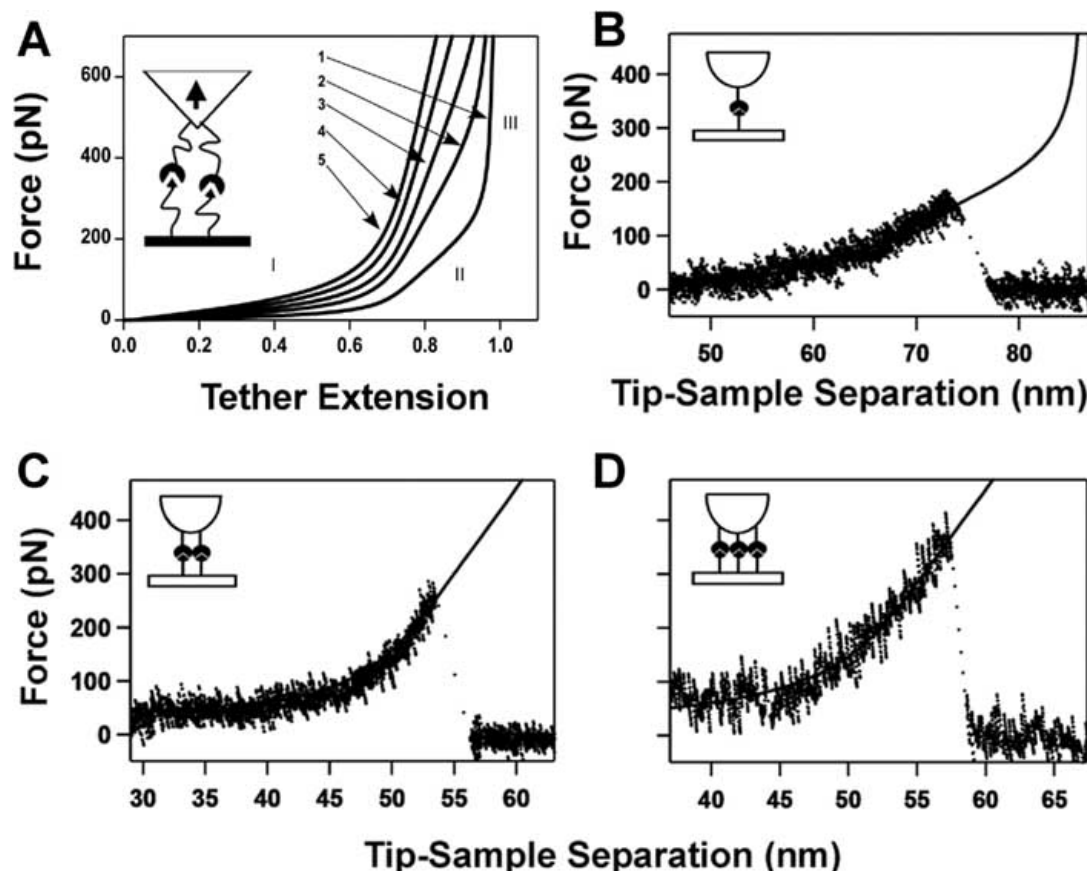


Fig. (4). A. Force-extension profiles calculated for several PEG linkers connected in parallel. B-D. Stretching traces for one, two, and three MUC1-scFv interacting pairs connected by PEG tethers. Solid lines indicate fits to the TLS-eFJC model.

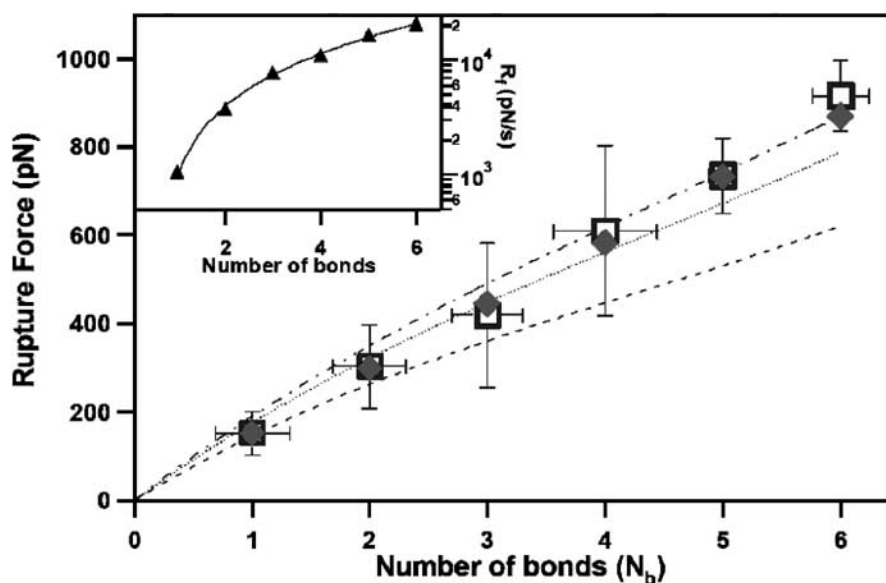


Fig. (5). Plot of the measured rupture forces (open squares, \square) as a function of the number of MUC1-scFv bonds between the AFM tip and sample. Solid diamond symbols (\blacklozenge) correspond to the rupture forces calculated using the Markovian model for the strength of multiple bonds using the average loading rate determined for each particular number of bonds. Lines correspond to the predictions of the same model using a single value of the average measured loading rate for 1 (dashed), 3 (dotted), and 6 (dash-dotted) bonds over the whole range of bond numbers. **Inset:** The average measured instantaneous loading rates (solid triangles, \blacktriangle) for the full range of bond numbers used in our experiments. Solid line is provided as a guide to the eye.

connections that need to be loaded by higher forces which then produce increased loading rates even if the AFM transducer retracts at a constant velocity. The net result is that the rupture events recorded in the experiments show a bias towards higher loading rates at higher bond number (Fig. 5, Inset). Indeed if we calculate the expected rupture force using the average loading rates for each number of bonds then the calculated forces match the experimental results over the entire range of the data (Fig. 5).

Interestingly, the apparent linear dependence of the measured rupture forces on the number of bonds seen in Fig. 5 can hint at the reasons why some AFM-based force measurements at first seem to match the predictions of the Poisson statistics model [30]. This method is based on the assumption that the rupture force for multiple parallel bonds scales linearly with the number of bonds; but this assumption is considered to be incorrect [29]. We note that in our experiments the “linear” scaling reflects the bias in loading rates specific to the AFM measurement with tethered ligands and not the fundamental scaling relationship for the strength of multiple bonds. Therefore, we stress that the Poisson statistics analysis will not produce a meaningful value for the single bond strength even in this case and researchers should use a full Markovian model [29] to analyze force spectroscopy measurements.

Dynamic Force Spectroscopy of Single and Multiple Tethered Bonds

The force spectroscopy measurements in tethered systems typically produce a continuous spectrum of loading rates due to coupling of the intentional variations in loading rate provided by changing the AFM cantilever retraction speed and the natural spread in loading rate values resulting

from the bond ruptures occurring at different points on the tether stretching curve. These variations provide the means to construct a plot of the measured rupture forces as a function of the logarithm of the instantaneous loading rate determined from the PEG elasticity fits. The dynamic force spectra obtained by this procedure (Fig. 6) shows the behavior predicted by Eq. 7 and other phenomenological descriptions [16]. The dynamic force spectrum for the rupture of single bonds indicates that the unbinding events observed in these experiments correspond to a potential energy barrier located at 2.8 ± 0.2 Å [31]. This value compares favorably with the bond distance of 2.6 Å, determined from the docking simulations of MUC1-antibody interactions [31]. The kinetic off-rate of $2.6 \cdot 10^{-3} \text{ s}^{-1}$ determined from the dynamic force spectrum (Table 1) also compares favorably with the $0.4 \cdot 10^{-3} \text{ s}^{-1}$ off-rate determined from bulk surface plasmon resonance (SPR) measurements. We note that the values of these rates can rule out the possibility of protein unfolding in our experiments: kinetic off-rates for scFv unfolding measured by bulk spectroscopy techniques [32] are two orders of magnitude slower than the off-rates measured in our experiments. In addition, Hinterdorfer and colleagues showed that forces required for breaking antibody-antigen interactions are much weaker than the forces required for antibody unfolding [33]. Our procedures for counting single bonds also allow construction of the dynamic force spectra for the rupture of different numbers of multiple bonds. Remarkably, a comparison of the force spectra for rupture of one, two and three bonds shows that they exhibit very similar distances to the transition state (Table 1). The effective kinetic off-rates for mono and multivalent MUC1-antibody interactions, determined by fitting the spectra to Eq. 1 (Table 1) show the expected large

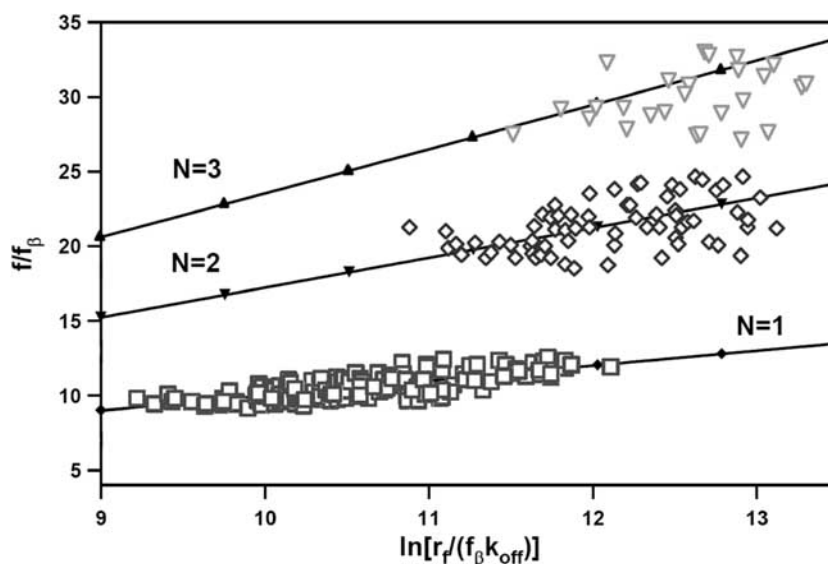


Fig. (6). Comparison of the normalized dynamic force spectra for the rupture of one (\square), two (\diamond), and three (∇) MUC1-antibody bonds with the prediction of the uncorrelated multiple bond rupture model. The experimental data were normalized according to Eq. 8. Solid lines represent the results of the numerical solutions of Eq. 9 for $N=1$ (\blacklozenge), 2 (\blacktriangledown), and 3 (\blacktriangle).

Table 1. Apparent values of the distances to the transition state, χ_β , kinetic off-rates, k_{off} , and the average bond lifetime $\tau_{off}=1/k_{off}$ determined using a single-bond approximation (Eq. 8 with $N=1$) [31]

	1 Bond	2 Bonds	3 Bonds
$\chi_\beta, \text{\AA}$	2.8 ± 0.2	2.0 ± 0.4	2.4 ± 1.5
k_{off}, s^{-1}	$2.6 \cdot 10^{-3}$	$7.2 \cdot 10^{-5}$	$3.6 \cdot 10^{-8}$
τ_{off}	284 s	3.8 hrs	320 days

drop in the kinetic off-rates with an increase in the number of bonds.

These data clearly illustrate that the main benefit of multivalent interactions is the reduction of the kinetic off-rate and the corresponding increase in the bond lifetime. Interestingly, these data point out a pathway for optimizing the design of multivalent radioimmunotherapeutics: researchers need to match the half life of the radioactive payload with the expected lifetime for the multivalent binding interaction. For instance, half-life time for the common radioactive payload Y^{90} is 65 hours; therefore an ideal multivalent targeting molecule featuring MUC1-targeting antibodies should link three scFv units to achieve the necessary binding efficiency.

These experimental data also allow testing of the general predictions of the theory of uncorrelated rupture of multiple parallel bonds. The uncorrelated failure mode implies no particular mechanical coupling between individual bonds and Williams showed that the force-induced rupture of such a connection could be described as a Markovian sequence [29]. To simplify the description we will use the normalization for force and loading rate [34]:

$$F = \frac{f}{f_\beta}; \quad R = \frac{r}{f_\beta k_{off}}; \quad (8)$$

where f_β is the thermal force scale defined as $k_B T / \chi_\beta$. The equivalent single bond approximation [29, 34] then produces the following expression relating the normalized loading rate R , to the most probable rupture force F^* and the number of bonds N :

$$R = \left[\sum_{n=1}^N \frac{1}{n^2} \exp\left(-\frac{F^*}{n}\right) \right]^{-1} \quad (9)$$

Rupture forces calculated from Eq. 9 (which is a normalized form of Eq. 7) show extremely good agreement with the experimental data (Fig. 6) demonstrating that the Markovian model [29] provides an accurate description of the dynamic failure of multiple uncorrelated parallel connections. In addition, analysis of the measured variations in the rupture forces also agrees with the predictions of the Markovian model [31].

CONCLUSIONS

We showed that use of long flexible tethers to connect interacting molecules to the surfaces of an AFM tip and sample provide several critical advantages for force spectroscopy experiments: the tethers identify specific binding interactions and separate them from the non-specific interactions; the elastic signature of the tether identifies the number of bonds independent of the measured rupture forces; and finally, the tethers suppress the rebinding process at any loading rate. These advantages allow researchers to construct accurate dynamic force spectra for the rupture of mono and multivalent interactions and quantify the advantages of the multivalent binding. Measured bond strength and the dynamic force spectra show excellent agreement with the Markovian model for the rupture of multiple uncorrelated molecular bonds, providing a solid experimental corroboration for the theoretical predictions.

Tethered ligand systems can serve as a flexible and versatile model for studying fundamental dynamics of individual bond rupture in biological systems. Multivalent binding is a common tool for molecular targeting that enables extended and more accurate delivery of drugs and molecular labels to specific tissues. Dynamic force spectroscopy measurements can provide an accurate measurement of the kinetic off-rates in such systems. These off-rates are the main determinant of the drug efficiency and quantification of the advantages of multivalent binding can provide a valuable input into the design efforts. Force spectroscopy techniques are especially useful for characterization of very strong interactions which could be difficult to observe on reasonable experimental time scales by other methods. These results could accelerate the efforts to design the next generation of superior multivalent binders for disease treatment and tissue imaging.

ACKNOWLEDGMENT

Funding from LLNL LSTO and UCD Cancer Center, RWF was supported by LLNL SEGRF program. This work was performed at the Lawrence Livermore National Laboratory under the auspices of the US Department of Energy under Contract No. W-7405-Eng-48.

REFERENCES

- [1] Cochran, J. R.; Cameron, T. O.; Stone, J. D.; Lubetsky, J. B.; Stern, L. J. *J. Biol. Chem.* **2001**, *276*(30), 28068-28074.
- [2] van Kooyk, Y.; Figdor, C. G. *Curr. Opin. Cell Biol.* **2000**, *12*(5), 542-547.
- [3] Mammen, M.; Choi, S. K.; Whitesides, G. M. *Angew. Chem.* **1998**, *37*(20), 2755-2794.
- [4] Holliger, P.; Prospero, T.; Winter, G. *Proc. Natl. Acad. Sci. USA* **1993**, *90*(14), 6444-6448.

- [5] Todorovska, A.; Roovers, R. C.; Dolezal, O.; Kortt, A. A.; Hoogenboom, H. R.; Hudson, P. J. *J. Immunol. Meth.* **2001**, *248*(1-2), 47-66.
- [6] Souriau, C.; Hudson, P. J. *Expert Opin. Biol. Ther.* **2003**, *3* (2), 305-18.
- [7] Rowland, G.; O'Neill, G.; Davies, D. *Nature* **1975**, *25*, (5508), 487-488.
- [8] Bustamante, C.; Macosko, J. C.; Wuite, G. J. L. *Nature Rev. Molec. Cell Biol.* **2000**, *1*(2), 130-136.
- [9] Clausen-Schaumann, H.; Seitz, M.; Krautbauer, R.; Gaub, H. E. *Curr. Opin. Chem. Biol.* **2000**, *4*(5), 524-530.
- [10] Noy, A.; Vezenov, D.; Lieber, C. *Ann. Rev. Mat. Sci.* **1997**, *27*, 381-421.
- [11] Merkel, R.; Nassoy, P.; Leung, A.; Ritchie, K.; Evans, E. *Nature* **1999**, *397*, 50-52.
- [12] Alon, R.; Hammer, D. A.; Springer, T. A. *Nature* **1995**, *374* (6522), 539-542.
- [13] Thoumine, O.; Kocian, P.; Kottelat, A.; Meister, J.-J. *European Biophysics Journal* **2000**, *29*(6), 398-408.
- [14] Florin, E. L.; Moy, V. T.; Gaub, H. E. *Science* **1994**, *264*(5157), 415-417.
- [15] Moy, V. T.; Florin, E. L.; Gaub, H. E. *Science* **1994**, *266*(5183), 257-9.
- [16] Evans, E.; Ritchie, K. *Biophys. J.* **1997**, *72*(4), 1541-1555.
- [17] Israelachvili, J. N.; McGuiggan, P. M. *Science* **1988**, *241*(4867), 795-800.
- [18] Svoboda, K.; Block, S. *Ann. Rev. Biophys. Biomol. Struct.* **1994**, *23*, 247-285.
- [19] Bell, G. I. *Science* **1978**, *200*(4342), 618-27.
- [20] Kienberger, F.; Pastushenko, V.; Kada, G.; Gruber, H.; Riener, C.; Schindler, H.; Hinterdorfer, P. *Single Molecules* **2000**, *1*(2), 123-128.
- [21] Kratky, O.; Porod, G. *Recueil des Travaux Chimiques des Pays-Bas* **1949**, *68*, 1106-1123.
- [22] Tskhovrebova, L.; Trinick, J.; Sleep, J.; Simmons, R. *Nature* **1997**, *387*, 308-312.
- [23] Oosterhelt, F.; Rief, M.; Gaub, H. E. *New J. Phys.* **1999**, *1* (1), 1-11.
- [24] Kramers, H. A. *Physica* **1940**, *7*, 284-304.
- [25] Jeffery, S.; Hoffmann, P. M.; Pethica, J. B.; Ramanujan, C.; Ozer, H. O.; Oral, A. *Phys. Rev. B* **2004**, *70*(5), 054114-8.
- [26] Jeppesen, C.; Wong, J. Y.; Kuhl, T. L.; Israelachvili, J. N.; Mullah, N.; Zalipsky, S.; Marques, C. M. *Science* **2001**, *293*(5529), 465-468.
- [27] Friedsam, C.; Wehle, A. K.; Kuhner, F.; Gaub, H. E. *J. Phys. - Cond. Matt.* **2003**, *15*(18), S1709-S1723.
- [28] Sulchek, T.; Friddle, R. W.; Noy, A. *Biophys. J.* **2006**, *90*(12), 4686-4691.
- [29] Williams, P. M. *Analytica Chimica Acta* **2003**, *479*(1), 107-115.
- [30] Williams, J. M.; Han, T. J.; Beebe, T. P. *Langmuir* **1996**, *12*(5), 1291-1295.
- [31] Sulchek, T. A.; Friddle, R. W.; Langry, K.; Lau, E. Y.; Albrecht, H.; Ratto, T. V.; DeNardo, S. J.; Colvin, M. E.; Noy, A. *Proc. Natl. Acad. Sci. USA* **2005**, *102*(46), 16638-16643.
- [32] Jager, M.; Pluckthun, A. *FEBS Lett.* **1999**, *462*, 307-312.
- [33] Kienberger, F.; Kada, G.; Mueller, H.; Hinterdorfer, P. *J. Molec. Biol.* **2005**, *347*(3), 597.
- [34] Evans, E.; Williams, P., In *Physics of Bio-Molecules and Cells*, Flyvbjerg, H.; Jülicher, F.; Ormos, P.; David, F., Eds. Springer and EDP Sciences: Heidelberg, **2002**; Vol. 75, pp. 187-203.